Published in final edited form as:

Arterioscler Thromb Vasc Biol. 2019 February ; 39(2): 188–199. doi:10.1161/ATVBAHA.118.311720.

Perivascular Adipocytes Store Norepinephrine by Vesicular Transport

Maleeha F. Ahmad[1], **David Ferland**[1], **Nadia Ayala-Lopez**[2], **G. Andres Contreras**[3], **Emma Darios**[1], **Janice Thompson**[1], **Alexander Ismail**[1], **Kyan Thelen**[3], **Adam J. Moeser**[3], **Robert Burnett**[1], **Arun Anantharam**[4], and **Stephanie W. Watts**[1]

[1]Department of Pharmacology and Toxicology, Michigan State University, East Lansing, MI

[2]Department of Laboratory Medicine, Yale University, New Haven, CT

[3]Department of Large Animal Clinical Sciences, Michigan State University, East Lansing, MI

[4]Department of Pharmacology, University of Michigan Medical School, Ann Arbor, MI

Abstract

Objective-—Perivascular adipose tissue (PVAT) contains an independent adrenergic system that can take up, metabolize, release, and potentially synthesize the vasoactive catecholamine norepinephrine. Norepinephrine has been detected in PVAT, but the mechanism of its protection within this tissue is unknown. Here, we investigate if PVAT adipocytes can store norepinephrine using the vesicular monoamine transporter (VMAT).

Approach and Results-—High-performance liquid chromatography identified norepinephrine in normal male Sprague Dawley rat aortic, superior mesenteric artery, and mesenteric resistance (MR) PVATs, and retroperitoneal fat. RT-PCR revealed VMAT1 and VMAT2 mRNA expression in MRPVAT adipocytes and stromal vascular fraction. Immunofluorescence demonstrated the presence of VMAT1 and VMAT2, and the co-localization of VMAT2 with norepinephrine, in the cytoplasm of MRPVAT adipocytes. A protocol was developed to capture real-time uptake of Mini 202, a functional and fluorescent VMAT probe, in live rat PVAT adipocytes. Mini 202 was taken up by freshly isolated and differentiated adipocytes from MRPVAT, and adipocytes from thoracic aortic and superior mesenteric artery PVATs. In freshly isolated MRPVAT adipocytes, addition of Rose Bengal (VMAT inhibitor), nisoxetine (norepinephrine transporter inhibitor), or corticosterone (organic cation 3 transporter inhibitor) significantly reduced Mini 202 signal. Immunofluorescence supports that neither VMAT1 nor VMAT2 is present in retroperitoneal adipocytes, suggesting that PVAT adipocytes may be unique in storing norepinephrine.

Conclusions-—This study supports a novel function of PVAT adipocytes in storing amines in a VMAT-dependent manner. It provides a foundation for future studies exploring the purpose and mechanisms of norepinephrine storage by PVAT in normal physiology and obesity-related hypertension.

Address for correspondence: Maleeha Ahmad, Department of Pharmacology and Toxicology, Michigan State University, 1355 Bogue St., Rm B447, East Lansing, MI 48824, Telephone: 517-897-4644, Fax: 517-353-8915, ahmadmal@msu.edu.

Disclosures

None.

Graphical Abstract

Proposed NE storage mechanism in PVAT adipocytes. NE enters the cell through the plasma membrane transporters OCT3 and NET. NE is stored in vesicles within the cytoplasm by VMAT. Diagram not to scale.

Keywords

Adipose tissue; adipocyte; norepinephrine

AHA Subject Codes:

Cell biology; hypertension; membrane transport; basic science research

Introduction

Perivascular adipose tissue (PVAT), the tissue surrounding the vasculature, plays an undeniably important role in vascular health and disease. PVAT's intimate association with the vasculature allows it to be a powerful modulator of vascular tone and blood pressure through the uptake and release of vasoactive substances that, in health, exert a largely anti-contractile effect on vessels.[1]

Only recently did our understanding of PVAT evolve to encompass more than its function as a connective tissue between vessels. In 1991, Soltis and Cassis discovered that the isolated rat thoracic aorta with the PVAT intact exhibits an increased contractile response to the indirect sympathomimetic tyramine, and a decreased sensitivity to the catecholamine norepinephrine (NE), a vasoconstrictor.[2] A few studies since then have provided evidence for a functional adrenergic system residing within PVAT, independent from sympathetic nerves.[3,4,5,6,7] In 2011, Vargovic et al. made the discovery that mesenteric PVAT contains, and can likely synthesize, catecholamines, most notably NE.[3]

Our previous studies demonstrate that PVAT adipocytes can take up,[5] metabolize,[6] and release[7] NE. Tetrabenazine, the classic VMAT inhibitor, decreased tyramine-induced contraction in aorta and superior mesenteric artery with PVAT.[7] This raised the question: can the PVAT adipocyte also store NE? We hypothesized that PVAT adipocytes *do* store NE, and that they use the vesicular monoamine transporter (VMAT) to do so, similar to sympathetic neurons.[8] A clearer understanding of the mechanism by which PVAT stores NE is crucial to fully appreciate the impact that PVAT's adrenergic system has on the vasculature.

To test this hypothesis, PVATs from around the rat thoracic aorta (TA), superior mesenteric artery and vein (SMA/V), and mesenteric resistance vessels (MRV) of the mesenteric arcade were used- APVAT, SMPVAT, and MRPVAT, respectively. These PVATs were chosen because the TA is an important conduit artery, and the SMA/V is the gatekeeper to the MRV, which are model resistance vessels.[6,7,9] Furthermore, these three PVATs consist of different types of fat. APVAT is composed of adipocytes similar to those found in brown adipose tissue, MRPVAT of adipocytes similar to white adipocytes, and SMPVAT is a mixture of

both.[10,11] As a white PVAT adipocyte model (MRPVAT adipocytes) was employed for our functional experiments, we predicted that VMAT is embedded in storage vesicles within the cytoplasm surrounding the large fat droplet and non-central nucleus of the cell typical of a white adipocyte.[12]

A multi-faceted approach was used to test this hypothesis. High-performance liquid chromatography (HPLC) was used to measure NE content in fats, RT-PCR to detect VMAT mRNA in PVAT adipocytes and SVF, and immunofluorescence for VMAT and NE imaging. The MRPVAT was our primary focus of these studies. We developed a novel assay using Mini 202 to test whether NE uptake and storage in MRPVAT adipocytes is dependent on specific transporters. Mini 202 is a VMAT-specific, pH-responsive fluorescent false neurotransmitter that has been utilized to demonstrate probe uptake in VMAT2-transfected human embryonic kidney (HEK) cells, and to measure the pH of catecholamine secretory vesicles in PC-12 (rat adrenal medulla pheochromocytoma) cells, which express VMAT1.[13] Importantly, Mini202 uptake was investigated in multiple adipocytes, namely those freshly isolated from TA, SMA/V and MRV, as well as MRPVAT adipocytes differentiated from precursor cells in MRPVAT SVF.

Our results support that a NE storage mechanism exists in the MRPVAT adipocyte, and that it is VMAT-dependent. These data help elucidate the independent adrenergic system within PVAT and set the stage for further research on how the obesity-related changes to this tissue can lead to hypertension.

Materials and Methods

The authors declare that all supporting data are available within the article [and its online supplementary files].

Materials

The fluorescent false neurotransmitter, Mini 202, was purchased from Abcam (cat. ab120867; Cambridge, MA, USA). Nisoxetine was purchased from Millipore-Sigma (cat. N151; Burlington, MA, USA), and Rose Bengal (cat. 5168) and corticosterone (cat. 3685) were purchased from Tocris Bioscience (Bristol, UK). Unless stated, all other chemicals were purchased from Millipore-Sigma. Please see the Major Resources Table in the Supplemental Material.

Animals

All protocols were approved by Michigan State University's Institutional Animal Care and Use Committee. Normal male Sprague Dawley rats (Charles River, Indianapolis, IN, USA) were used in accordance with the Guide for the Care and Use of Laboratory Animals (8th edn, 2011). The PVATs investigated have qualitatively and quantitatively similar magnitudes of catecholamine content when comparing specific tissues from male *vs* female. As such, the male was chosen as an overall model. The total number of rats used was 68. Rats were anesthetized with pentobarbital (80 mg kg^{-1} intraperitoneal), decapitated, exsanguinated, and tissues were removed. The fat located directly adjacent to the vessel was considered to be each respective PVAT (APVAT, SMPVAT, MRPVAT), and was dissected in buffered

solution with the aid of a stereomicroscope and micro scissors. Retroperitoneal (RP) fat was removed from behind the kidneys. Adrenal medullae dissection is expanded upon below.

High-performance liquid chromatography

APVAT, SMPVAT, MRPVAT, and RP fat tissues were homogenized in four times their weight of 0.1 M percholoric acid, centrifuged, and run through a 30 kDa filtration tube. The filtrates were analyzed on an HPLC system with a Coulochem III electrochemical detector set at −300 mV (Thermo Fisher Scientific; Waltham, MA, USA). Analytes were separated at 35°C on a HR-80 reverse-phase column (Thermo Fisher Scientific) with Cat-A-Phase II (Thermo Fisher Scientific), a mobile phase with a flow rate of 1.1 mL min^{-1}. Standards were run every 5th sample to confirm peak location on the chromatogram. The limit of detection for NE was 0.1 ng mL^{-1}. HPLC data are reported as the mean ± SEM NE content in each tissue.

RT-PCR

MRPVAT adipocytes and SVF were isolated from the PVAT as described previously.[14] Adrenal medullae and the locus coeruleus of the brain were used as positive controls for VMAT1 and VMAT2, respectively. The adipocytes and tissues were homogenized with an Omni Bead Ruptor (Omni Inc; Kennesaw, GA, USA) with the following parameters: 2 cycles for 30 s at speed 5.65 with 30 s delay between cycles, all at 6°C. RNA was extracted using the Quick RNA MiniPrep kit (Zymo Research, cat. R1054; Irving, CA, USA). The DNase within the Zymo kit (cat E1010, DNase I set) was used to remove genomic DNA. RNA purity (260/280 and 260/230 ratios ≥ 1.8) was assessed with a Nanodrop 2000C spectrophotometer (Thermo Fisher Scientific). mRNA was reverse transcribed with a High Capacity cDNA Reverse Transcription kit (Thermo Fisher Scientific). Taqman primers for Slc18a1 (VMAT1; cat. Rn00461866_m1, Thermo Fisher Scientific) and Slc18a2 (VMAT2; cat. Rn00564688_m1, Thermo Fisher Scientific) were used. RT-PCR was performed using Taqman PerFecta FastMix (Quanta Bioscience; Beverly, MA, USA) on the ABI 7500 Fast Real-Time PCR system with the following parameters: 40 cycles of 95°C for 20 s, then 40 cycles of 95°C for 1 s, and 60°C for 20 s. Measures were compared to the house-keeping gene beta-actin (cat. Rn00667869_m1; Thermo Fisher Scientific). Controls without RT were run so as to confirm the lack of genomic DNA in the amplified sample. RT-PCR results are reported as cycle threshold (C_T) values out of 40 cycles and normalized to beta-actin.

Immunofluorescence

All tissue sections were formalin-fixed and paraffin embedded. TA + PVAT, SMA/V + PVAT, and MRV + PVAT were embedded and sectioned (8 μm thick) by Michigan State University's Investigative Histopathology Lab. Rat whole adrenal, coronal brain (region 4), and RP fat sections (5 μm thick) were purchased from Zyagen (San Diego, CA, USA). Adrenal medulla and the anterior commissure or caudate putamen region of the brain were used as positive controls for VMAT1 and VMAT2, respectively. Using standard IHC protocols, slides were de-waxed, antigens unmasked, and sections encircled with a hydrophobic barrier pen. Sections were rinsed three times for five minutes each with PBS with 0.1% Triton X-100 (PBS-TX), as were all subsequent washes. All sections were incubated in a species-specific blocking serum (BS-Tx: 1.5% goat serum in PBS-TX; Vector

Laboratories, Burlingame, CA) for 60 minutes at room temperature. Experimental sections were then incubated with the VMAT1 primary antibody (rabbit; 1:500 in BS-TX; cat. 20041; Immunostar; Hudson, WI, USA) or the VMAT2 primary antibody (rabbit; 1:250 in BS-TX; cat. 20042; Immunostar) overnight at 4°C. Parallel sections were incubated in BS-TX. All sections were then washed, incubated with the Alexa Fluor 488 fluorescent secondary antibody (Alexa Fluor 488 goat anti-rabbit; 1:1000; cat. A11008; Thermo Fisher Scientific) at room temperature for 60 minutes and washed again. ProLong Gold Anti-fade Mountant with DAPI (cat. P36931, Thermo Fisher Scientific) was applied to all sections. Slides were coverslipped and subsequently imaged using a 100× objective on a Nikon Eclipse TE2000 inverted microscope (Nikon Group, Otowara, Japan). Fluorescent images were captured using a Nikon Digital Sight DS-Qil camera and Nikon NIS Elements BR 3.00 software. Adjustments in brightness and contrast for all fluorescent images were applied uniformly across each image, and relative to each sample's negative controls, using Photoshop CS6 v. 13.0 ×64 (Adobe Systems, San Jose, CA). Images representative of at least four animals were selected for the figures.

Co-localization immunofluorescence

The above protocol was followed with the following adjustments. Rat SMA/V + PVAT and MRV + PVAT were the experimental sections, and rat coronal brain and whole adrenal sections were used as positive controls. All sections were incubated in a species-specific blocking serum (1.5% rabbit serum in PBS-TX) for 60 minutes at room temperature. Experimental sections were then incubated with a VMAT2 primary antibody (goat; 1:100 in BS-TX; cat. NB100–1479; Novus Biologicals; Littleton, CO, USA), while parallel sections were incubated in BS-TX, overnight at 4°C. All sections were rinsed, incubated in the Alexa Fluor 568 fluorescent secondary antibody (Alexa Fluor 568 rabbit anti-goat; 1:1000; cat. A11079; Thermo Fisher Scientific) at room temperature for 60 minutes and washed again. Sections were then blocked in a second species-specific blocking serum (1.5% goat serum in PBS-TX) for 60 minutes at room temperature. Experimental sections were next incubated with a NE primary antibody (rabbit; 1:50; cat. Ab8887; Abcam), while parallel sections were incubated in BS-TX, overnight at 4°C. All sections were washed, incubated with the Alexa Fluor 488 fluorescent secondary antibody (Alexa Fluor 488 goat anti-rabbit; 1:1000) at room temperature for 60 minutes, and washed again. Slides were imaged using a 120× objective on an Olympus FluoView FV1000 Confocal Laser Scanning Microscope (Olympus Corporation, Tokyo, Japan). Fluorescent Z-stack images were captured using a FluoView FV1000 ASW Version 4.0 software (Olympus). For co-staining immunofluorescence experiments, co-localization of NE and VMAT2 was determined by the presence of yellow fluorescence. Adjustments in brightness and contrast for all fluorescent images were applied uniformly across each image, and relative to each sample's negative controls.

Mini 202 functional experiments

This protocol was adapted for application in adrenal medulla chromaffin cells (Mini 202 positive control) and adipocytes from Lee et al.'s procedure (detailed in their supplemental materials).[13]

Adrenal medulla chromaffin cells: The adrenal glands from two euthanized rats (8–12 weeks) were removed and transferred into dishes containing ice-cold dissection buffer (148 mM NaCl, 2.57 mM KCl, 2.2 mM K_2HPO_4•$3H_2O$, 6.5 mM KH_2PO_4, 10 mM glucose, 5 mM HEPES free acid, 14.2 mM mannitol). The cortices were carefully trimmed away and the isolated medullas were digested (2 times 15 min at 37°C, oscillating) in 1 mL of enzyme solution containing 600 units papain (Papain suspension; cat. LS003126; Worthington Biochemical, Lakewood, NJ), 500 μg BSA, and 150 μg dithiothreitol. The digested glands were then suspended in Dulbecco's Modified Eagle's Medium (DMEM; Thermo Fisher Scientific) supplemented with 10% fetal bovine serum (FBS; Thermo Fisher Scientific) and triturated by a push-pull movement through a 1 mL pipette tip (10 to 15 times). The solution was then spun at 1200 × g for 2.5 minutes. The supernatant was discarded, the pellet re-suspended in DMEM + 10% FBS and triturated again in a 200 μL pipette tip for better cell dissociation. Seventy-five μL of cell suspension were plated in wells of a Collagen IV-coated 8 well chamber slide (μ-Slide 8 well; cat. 80822; Ibidi; Planegg, Germany) and 125 μL DMEM + 10% FBS were added to each well. Cells were incubated (90 min at 37°C, 5% CO_2) to allow for settling and attachment. Mini 202 (500 μM) was added to one well and incubated for 60 min. Solutions were then aspirated and cells washed three times with DMEM + 10% FBS. Two-hundred μL DMEM + 10% FBS were added to each chamber and cells were imaged using a 40× objective and the same microscope, camera, and software described previously. Mini 202 signal was visible in the DAPI channel with a SOLA light engine (Lumencor Inc., Beaverton, OR, USA).

Adipocytes:

MRPVAT adipocytes: The mesenteries were removed from two euthanized rats (350 to 430 g in weight) and tissues pooled to constitute a biological N=1. Mesenteries were cut into 3–4 pieces and the intestinal contents were evacuated from the intestine to avoid contamination of the PVAT. Tissues were kept and dissected in chilled Krebs-Ringer Bicarbonate Buffer (KRBB; 135 mM NaCl, 5 mM KCl, 1 mM $MgSO_4$, 0.4 mM K_2HPO_4, 5.5 mM glucose, 20 mM HEPES, 10 mL antibiotic/antimycotic. pH to 7.4). MRPVAT was dissected from around the MRV using a stereomicroscope and collected in chilled KRBB.[14] Dissected PVAT was added to tubes with 1 mL of warmed digestion solution containing 1 mg of collagenase (collagenase Type I; cat. LS004196; Worthington Biochemical) and 4% bovine serum albumin (BSA; cat. A2153; Sigma) in KRBB. Small scissors were used to mince the tissue. The samples were then placed at 37°C in a rotating incubator at low speed for 60 min or until the solution appeared "milky" and no large PVAT fragments were visible. The tubes were centrifuged at 200 × g for 5 min, and the SVF that pelleted to the bottom was discarded. Adipocytes were washed three times with 1 mL of warm wash solution (4% BSA in KRBB). All adipocytes were then combined, and the total volume measured.

For adipocytes from MRPVAT, this volume was evenly split amongst three 1.5 mL tubes. Vehicle and KRBB were added to the first and second tubes. Inhibitor (100 μM Rose Bengal,[15] VMAT; 1 μM nisoxetine, NET; or 1 mM corticosterone, OCT3) and KRBB were added to the third tube. For all incubations in the nisoxetine experiments, the KRBB in each condition contained 1% BSA to aid in inhibitor suspension and delivery to the cell. All tubes were incubated for 30 min at 37°C with rotation. Mini 202 (500 μM) was added to the

second and third tubes, and all tubes were further incubated for 60 minutes in the dark. A concentration of 500 μM Mini 202 was selected because it produced consistent signal while avoiding camera saturation. All cells were centrifuged and washed with wash solution three times, as before. Twenty μL of adipocytes were then plated on an uncoated Ibidi μ-slide Angiogenesis slide (cat. 81506; Ibidi) and imaged as described for chromaffin cells. The full experimental protocol is depicted in Figure 1.

The unadjusted fluorescent TIFF images were quantified on Image Studio (LI-COR Biosciences; Lincoln, NE, USA) in duplicate by two independent researchers. Two concentric circles were drawn to enclose the signal around the edge of each cell and to set the inside of each cell as its own baseline due to the varying background intensities of floating cells. Two independent researchers quantified all cells in the images that were in focus with consistent methods as their overall means did not differ significantly. Each researcher's mean of the arbitrary signal intensities for each condition was calculated per experiment. These means were then averaged with their pairs to obtain four means (N=4) per condition. The images selected for display were representative of all (biological N=4) images in that treatment condition.

TA and SMA/V adipocytes: In a separate experiment using adipocytes isolated from MRPVAT (for comparison), TA, and SMA/V PVAT, incubation with Mini202 (500 μM) was performed compared to a vehicle control so as to determine the generality of Mini202 uptake between adipocytes isolated from different vessels. Isolation and staining occurred exactly as described above. Cellular images were captured and analyzed on the Nexcelom Cellometer Vision® (Nexcelom Bioscience, Lawrence, MA) with the 450–302 cube. In these same cells, the viability of the adipocytes was assessed by uptake of the nucleic acid binding dyes acridine orange (AO) and propidium iodide (PI) (Cellometer AOPI #CS2–0106, Nexcelom Bioscience). AO is cell permeable (nuclear) and PI will only enter a cell with a compromised membrane, or an unhealthy/dying, dead or necrotic cells. Adipocytes from these experiments were imaged using the Cellometer Vision, 535–402 cube, 660–502 cube and data analyzed using Cellometer Vision software v.2.1.10.11.

Adipocytes differentiated from MRPVAT SVF: Preadipocytes were obtained from MRPVAT SVF after two serial passages in culture flasks (Nest Biotechnology, Rahway, NJ, USA) as reported.[16] Expanded preadipocytes populations were seeded in 24 well plates (Corning) at a concentration of 20,000 cells/cm^2 and allowed to proliferate to confluency. Preadipocytes were then induced to differentiate using standardized adipogenic media while in coculture with primary MRPVAT adipocytes (900 cells/cm^2) contained in a 0.4 μm trans-well insert (Greiner Bio-One).[16] Primary adipocytes were removed after 5 days of coculture and differentiated cultured adipocytes were used two days later for Mini 202 functional experiments. Cells were imaged as described above for chromaffin cells.

Immunocytochemistry

MRPVAT adipocytes and corresponding SVF were isolated as stated above. For CD68 staining, cells were incubated for 1 hour at 37°C with mouse anti-rat CD68 (1:50, #MCA341, Bio-Rad, Hercules, CA), washed three times (4% BSA in KRBB), and incubated

for 30 minutes at 37°C with goat anti-mouse Alexa Fluor 488 (1:1000, A11029, Thermo Fisher Scientific). After two additional washes (4% BSA in KRBB), cells were loaded into the Cellometer Vision® and images captured with the 535–402 cube and brightfield microscopy. Fluorescent images (raw 8-bit) were imported to ImageJ v.1.48a, thresholded to remove background, colorized to red, and overlaid on the corresponding brightfield image to view co-localization with adipocytes.

MR, TA, and SMA/V adipocytes were isolated as stated above. Cells were incubated with 1 mg/mL of WGA Alexa Fluor-555 (W32464, Thermo Fisher Scientific) for 10 minutes at 37°C. After two washes (4% BSA in KRBB), cells were imaged on the Cellometer Vision® with the 595–502 cube. In copies of these images, brightness was enhanced for better visibility.

Differentiated adipocytes were isolated as described above. Cells were fixed with 4% paraformaldehyde in PBS overnight then washed once with PBS. Cells were then stained for VMAT1 and VMAT2 as stated above in *Immunofluorescence*.

To stain lipid, fixed cells were treated with the neutral lipid stain HCS LipidTox™ (H34477, Life Technologies, Carlsbad, CA, USA) using 300 microliters of a 1:1000 dilution per cm^2 of tissue culture area. For counterstaining, NucBlue™ (R37605, Thermo Scientific) was used following manufacturer's instructions.

Statistical Analyses

All values reported represent means±SEM for the number of biological replicates represented by N. Variables were tested for normality (Kolmogorov-Smirnov) and homogeneity of variances before application of the appropriate statistical test.

HPLC: The equality of the variances for the mean values was verified with the Bartlett test after an arcsine transformation to account for the non-Gaussian RP fat data. A one-way ANOVA with post-hoc Bonferroni's test was performed on these values, and a $P < 0.05$ was considered statistically significant. The graph of these data represents actual NE content in ng g^{-1} tissue, but statistical significance is the same as for the transformed values.

Mini 202 experiments + inhibitors: These data were transformed by adding the absolute value of the lowest mean to all other means to account for the several negative signal intensities found in the vehicle and inhibitor conditions (when the background of the well was often brighter than the perimeter of the cell itself). The equality of the variances for the resulting mean values was verified with the Brown-Forsythe test. A one-way ANOVA with post hoc Bonferroni's test was then used to determine statistical significance between conditions. The data are presented as mean ± SEM arbitrary signal intensities, with a $P < 0.05$ considered statistically significant.

Results

PVATs contain NE

HPLC was used to measure NE content in the PVATs surrounding the thoracic aorta (APVAT), superior mesenteric artery and vein (SMPVAT), and the mesenteric resistance vessels of the mesenteric arcade (MRPVAT). Figure 2 shows that all three PVATs contain notable levels of NE (APVAT= 739.98 ± 15.78 ng g^{-1} tissue; SMPVAT= 364.72 ± 44.06 ng g^{-1} tissue; MRPVAT= 96.17 ± 23.90 ng g^{-1} tissue), although content varies significantly between all PVATs. NE is also detectable in RP fat (RP fat= 44.104 ± 3.89 ng g^{-1} tissue) but at a lower concentration than it is in PVAT tissues. These data support that NE is present in PVAT. The PVAT adipocyte was the logical place to begin investigating a potential NE storage mechanism.

Mesenteric PVATs and PVAT adipocytes contain VMAT; RP fat does not

PCR: mRNA for VMAT1 and VMAT2 was detected at low but measurable levels in MRPVAT adipocytes and in SVF from the same PVAT (Table 1). The positive controls for VMAT1 (adrenal; C_T value 24.46) and VMAT2 (locus coeruleus; C_T value 26.95) validated proper detection of gene expression using these primers (Table 1). In a separate experiment using adipocytes only and performed by a different individual than was responsible for the data in Table 1, we observed a similar outcome (β-actin = 19.11±0.5; VMAT 1 = 36.72±0.71; VMAT2 = 33.98±0.32; N=4–5). We attempted Western analyses to compare the relative expression of these two VMAT proteins but were unsuccessful in procuring an antibody that could detect VMAT at the expected molecular weight. Thus, we turned to immunohistochemistry for which antibodies have been successfully developed for VMAT localization.

Immunofluorescence: For NE to be detectable, it must be protected in the cell. We hypothesize NE is stored in vesicles within the cytoplasm through VMAT as this is how sympathetic neurons store NE. Immunohistochemical staining revealed APVAT, SMPVAT, and MRPVAT contain VMAT1 (Figure 3A) and VMAT2 (Figure 3B). Positive staining for both these transporters is present surrounding the lipid of the adipocytes. In adipocytes differentiated and cultured from adipocyte precursors found in MRPVAT SVF, VMAT1 and VMAT2 staining can also be seen in the cytoplasm of the cell (Figure 3C). Interestingly, results indicate the absence of VMAT1 (Figure 3A) and VMAT2 (Figure 3B) from RP fat. Staining in rat adrenal medulla chromaffin cells and in the anterior commissure of the rat brain verified our ability to visualize VMAT1 and VMAT2, respectively, in the aforementioned tissues. Arrows point to areas of intense staining, many sites of which are near the nucleus. We have not stained for other organelles, so the precise cellular location of VMAT cannot be determined.

VMAT2 and NE co-localize in mesenteric PVATs

The higher expression of VMAT2 than VMAT1 mRNA in MRPVAT adipocytes directed the focus to VMAT2 for these co-localization experiments. Immunofluorescence experiments with antibodies against VMAT2 and NE demonstrated their co-localization in SMPVAT and MRPVAT. Arrows point to yellow signal in Figure 4, indicating areas of co-localization of

VMAT2 and NE. The caudate putamen region of the rat brain was used as a positive control, and co-localization in this tissue can be observed mainly around the nuclei. Macrophages, as stained by CD68, were not significantly associated with isolated adipocytes (supplemental figure I) and thus are an unlikely source of NE. These data thus far indicate that the PVAT adipocyte may be capable of storing NE *via* VMAT. Functional experiments were next performed in the isolated PVAT adipocyte to test this idea.

Inhibitors of plasma membrane transporters and VMAT decrease Mini 202 uptake in MRPVAT adipocytes

Adrenal medulla chromaffin cells: Chromaffin cells were isolated from rat adrenal medullae and used as a positive control for Mini 202 uptake. As shown in Figure 5A, cells were either incubated in vehicle (left) or Mini 202 (right). Arrows indicate only those cells that appear healthy (non-granulous cytoplasm). The presence of blue signal demonstrates chromaffin cells are capable of taking up Mini 202.

MRPVAT adipocytes: Adipocytes were isolated from the PVAT surrounding the mesenteric resistance vessels of the mesenteric arcade (MRPVAT). The plasma membrane of adipocytes remains intact through collagenase digestion (supplemental figure II). As shown in Figure 5B, cells were either incubated in vehicle (left), Mini 202 (middle), or an inhibitor and Mini 202 (right). These were inhibitors of VMAT (Rose Bengal, top), or of the plasma membrane transporters NET (nisoxetine, middle) and OCT3 (corticosterone, bottom). As indicated by arrows, treatment with the fluorescent false neurotransmitter Mini 202 resulted in a circle of blue signal around the lipid droplet of the cells that was brightest surrounding the nucleus (images taken microscopically). Not all cells were labelled with Mini 202, likely because cells were out of imaging focus, were lodged within clumps in which inner cells were not exposed to Mini 202,3 or were not viable. Test of cell viability using AO/PI indicate that cell viability was ~60–65% after collagenase digestion and at the time of experimentation. This value did not change in cells upon incubation with Mini 202 (supplemental figure III, open circles) or exposure to the inhibitors (e.g. nisoxetine = 56 ± 9% viability, N=3).

Treatment with the transporter inhibitors reduced this fluorescence. Figure 5C depicts the mean ± SEM for the signal intensities (SI), reported in arbitrary units, of the cells in these various conditions obtained through quantification with ImageStudio software. Rose Bengal treatment reduced Mini 202 SI from $2.07\times10^7 \pm 0.16\times10^7$ to $0.42\times10^7 \pm 0.10\times10^7$, or by 79.78 ± 5.16%. Nisoxetine treatment reduced Mini 202 SI from $2.17\times10^7 \pm 0.023\times10^7$ to $0.66\times10^7 \pm 0.043\times10^7$, or by 69.57 ± 2.00%. Corticosterone treatment reduced Mini 202 SI from $2.86\times10^7 \pm 0.13\times10^7$ to $1.10\times10^7 \pm 0.059\times10^7$, or by 61.48 ± 2.69%. The differences in arbitrary signal intensity between vehicle and Mini 202 conditions, and Mini 202 and inhibitor conditions were all significant by a one-way ANOVA, with P values of 0.0013 (* in Figure 5C) or < 0.0001 (** in Figure 5C). Uptake of Mini 202 was observed in adipocytes isolated from the SMA/V PVAT and TA PVAT (supplemental figure IVB, IVC; captured on the Vision® Cellometer) and MRPVAT adipocytes differentiated from adipocyte progenitor cells by primary adipocyte cell incubation (supplemental figure VA; taken microscopically). In the images procured on a Vision ®Cellometer, the halo of Mini 202 staining is less

evident. However, the qualitative similarity of Mini 202 uptake by adipocytes from MRPVAT as imaged in these two different ways, the microscope vs Cellometer, supports the conclusion that adipocytes from multiple PVATs can take up Mini 202. The presence of lipid in the differentiated adipocytes was confirmed by staining with LipidTox (supplemental figure VB).

Discussion

This is the first study to reveal VMAT presence and function in PVAT adipocytes. Taken together, these data provide evidence for a NE storage mechanism in the PVAT adipocyte. This mechanism involves NE uptake into the cell through the plasma membrane transporters NET and OCT3. Once in the cytosol, NE is taken up through VMAT for storage in vesicles (Figure 6).

Our data supports previous findings that PVAT contains functional catecholamines.[7] The analyzed PVATs contained NE, with APVAT and SMPVAT having over seven and three times more NE than MRPVAT, respectively (Figure 2). Although MRPVAT contains the least amount of NE of these PVATS, the functional experiments in this study were performed with these adipocytes because the MRV, being model resistance vessels, directly impact total peripheral resistance, and thus blood pressure.[9,17] Additionally, studies have shown positive correlation between increased visceral fat, like MRPVAT, and hypertension and cardiovascular risk.[18,19,20]

There are several reasons why the NE content of these tissues could be different from one another. The TA-PVAT, as a brown fat, was expected to be high in NE concentration given that brown fat is considered to be thermogenically driven by the sympathetic nervous system.[21] However, the TA itself is considered to be poorly innervated by the sympathetic nervous system[22] and has poor responses to electrical field stimulation.[23] This suggests that brown fat maintains catecholamine content either through synthesis or uptake from exogenous sources. In contrast, the RP fat had a substantially lower NE content, yet is known to be innervated by the sympathetic nervous system.[24] The magnitude of NE in SMPVAT is in between that of APVAT and RP fat. We have demonstrated that denervation of this tissue by celiac ganglionectomy did not abolish NE content.[7] Collectively, this evidence suggests it is more likely a property of the fat itself, as opposed to innervation, that influences final NE content. NE content could also be different between these tissues because of increased activity of NE metabolizing enzymes. Oxidases such as MAO, but more so semicarbazide sensitive amine oxidase (SSAO), are expressed in MRPVAT[6], specifically in the adipocytes of these tissues. SSAO was more highly expressed and functional in the MRPVAT *vs* MAO in an amine oxidase activity assay. MAOA and MAOB were virtually inactive in MRPVAT and MRPVAT adipocytes. If this is consistent between fats, SSAO expression and function could influence NE concentration. However, incubation of tissues with the SSAO inhibitor semicarbazide did not increase NE content in the TA or MRPVAT PVATs (not shown). While we have not done the comparative measures of SSAO expression and activity between the three PVATS – aortic, superior mesenteric and mesenteric resistance – and thus cannot exclude the possibility that oxidases may contribute

to the different concentration of NE in these tissues, our findings suggest the difference in NE concentration between fats is intrinsic to each PVAT.

The SMPVAT has smaller and more brown or multilocular adipocytes than MRPVAT, which is more flocculent and “white” in appearance. Macroscopically, MRPVAT resembles RP fat. However, this study determined that although RP fat contains NE (Figure 2), unlike PVAT, it does not contain VMAT1 or VMAT2 (Figure 3). Adipose tissues that are high in catecholamine content (APVAT and brown fat pad) are also positive for the brown adipose marker UCP1 (uncoupling protein 1).[11] These findings suggest that adipose tissues high in NE have more brown adipocyte-like characteristics and those with low NE content are more similar to white adipose tissue adipocytes.

MRPVAT adipocytes separated from the other components of PVAT contain NE.[5] NE content in PVAT occurs because of uptake of exogenous NE and may also be attributed to endogenous NE synthesis, as others have reported adipose tissue adipocytes as a potential source of catecholamine synthesis.[3] Macrophages have recently gained attention as cell types able to catabolize[25, 26], but not synthesize[27] NE. In our hands, CD68 positive cells are rarely associated with adipocytes and likely do not account for significant amounts of the NE measured in PVAT. Fischer et al concluded that “…macrophages do not synthesize relevant amounts of catecholamine, and hence are not likely to have a direct role in adipocyte metabolism or adaptive thermogenesis”.[27] It remains to be seen whether the uptake of exogenous NE and/or catabolism of NE by the macrophage could influence lipolysis, an endpoint that was not the focus of this work.

Rat APVAT and MRPVAT adipocytes can take up NE.[5] OCT3 is involved in the uptake of NE into PVAT adipocytes in the rat[5] and in human brown adipose tissue (BAT) biopsies.[28] In the present study, Mini 202 signal was present, supporting the function of VMAT in these tissues. Importantly, uptake of Mini 202 was observed not just in the adipocytes from MRPVAT, but also from TA and SMA/V PVAT adipocytes and adipocytes that underwent no collagenase digestion (cultured adipocytes). Collectively, these experiments support that there is a potential to store catecholamines in each of these adipocytes.

Mini 202 staining was inhibited by the OCT3 inhibitor corticosterone and the NET inhibitor nisoxetine (Figures 5 B,C). This suggests that Mini 202 enters the cell through OCT3 and NET and inhibiting entry through these transporters prevents its later interaction with VMAT. In MRPVAT, nisoxetine can completely inhibit the anti-contractile effect that PVAT has on mesenteric resistance vessels suggesting that PVAT acts as a sink for exogenous NE.[6]

VMAT1 and 2 are encoded by genes *SLC18A1* (on chromosome 8) and *SLC18A2* (on chromosome 10), respectively. Both genes exhibit high sequence homology. Both VMATs are ~70 kDa acidic glycoproteins that are predicted to have 12 transmembrane domains.[29] VMAT1 is usually found in the large dense core vesicles of neuroendocrine cells and VMAT2 in the CNS, mast cells, gut histamine-containing cells, and pancreatic beta-cells.[29] Interestingly, both were located in SM- and MRPVAT (Figure 3). The localization of the transporters in different tissues is species-dependent. However, mechanisms of NE uptake through OCT3 are conserved between the rat and human.[5,28] Although the amine 5-

hydroxytryptamine (5-HT) has a similar affinity for VMAT1 and VMAT2, the catecholamines dopamine (DA), NE, and epinephrine (E) have a 3-fold higher affinity for VMAT2.[29,30] The uptake efficiencies of these amines by VMAT2 is as follows: 5-HT> DA> E> NE.[29]

Prior to this study, little was known about VMAT in adipose tissue. 3T3-L1 adipocytes were recently discovered to express VMAT1, suggesting adipocytes have the ability to store amines.[14] Furthermore, 3T3-L1 adipocytes can take up NE.[14] However, tyramine (which causes the release of amines from intracellular stores through reverse transport) was unable to stimulate NE release, probably related to the finding that 3T3-L1 adipocytes do not express the plasma membrane transporters which are necessary for tyramine's function.[14] In contrast to 3T3-L1 adipocytes, rat MRPVAT adipocytes contain basal levels of NE and express OCT3.[5,14] Addition of tyramine on MR- and APVAT causes the release of NE, DA and 5-HT from the tissue,[7] different from what was observed in 3T3-L1 adipocytes.[14] Tyramine-stimulated release of catecholamines results in contraction of the isolated rat aorta and mesenteric artery only when the associated PVAT is left intact. Furthermore, tyramine's effect on contraction remained even after the neuronal innervation to the mesentery was removed by celiac ganglionectomy.[7] Addition of the VMAT inhibitor tetrabenazine reduced the maximal contraction to tyramine of the rat aorta with PVAT.[7] Together, those studies suggested that tyramine's effect was PVAT- and VMAT- dependent but nerve-independent.

PVAT contains cells other than neurons which could have functional VMATs and store NE. Human monocyte-derived macrophages express mRNA for DAT and VMAT2.[31] Mouse perivascular macrophages also express SERT.[32] However, the co-localization of VMAT2 with NE by confocal microscopy under high power clearly shows their presence in the cytoplasm of the PVAT adipocyte and not in other cells (Figure 4). Similarly, the minimal 'stickiness' of the macrophage to the isolated adipocytes suggests macrophages are not an important contributor of NE to the measures made.

We recognize that VMAT staining within the capillaries of the PVAT could compromise part of the staining observed, though a tissue like RP, which possesses capillaries, did not stain for VMAT1 or VMAT2. This is why experiments with the isolated adipocytes were critical, and they support both Mini202 uptake and staining for VMAT1 and VMAT2 in these cells.

Technical comments

The ability to conduct a functional assay with primary isolated MRPVAT adipocytes presented specific challenges. One reason for this is that primary adipocytes are fragile and prone to lysis once removed from their tissue matrix. Experiments ex-vivo with adipocytes have to be done quickly after isolation and with minimal manipulation of the adipocytes in order to prolong their health. Due to these limitations, functional assays are sometimes replaced with the use of adipocyte cell line models, such as 3T3-L1 mouse embryonic fibroblasts that are differentiated in vitro into cells that accumulate lipid and thus mimic adipocytes. We were able to do such experiments with a significant portion (~65%) of cells viable at the time of experimentation.

Another way to study adipocyte biology is by the isolation of primary pre-adipocytes that are then differentiated in culture to adipocytes before they are studied, and this is precisely what was done with adipocytes differentiated from the SVF of MRPVAT. The functional assays performed in this study utilized either primary PVAT adipocytes or adipocytes differentiated from SVF. The qualitatively similar finding of Mini 202 uptake by these adipocytes added confidence in the findings that VMAT is present in PVAT adipocytes and is functional.

Limitations

There is evidence to support that Mini 202 has reasonable specificity to VMAT1 and 2. Mini 202 is a substrate of VMAT1 (PC-12 cells) and VMAT2 tested in HEK cells stably expressing VMAT2.[13] Furthermore, Mini 202 staining was inhibited by reserpine in PC-12 (rat pheochromocytoma) cells and by reserpine and tetrabenazine in VMAT2 expressing HEK cells.[13] Transmission electron microscopy (TEM) would be the preferred method for NE/VMAT2 co-localization as it would allow for the visualization of the vesicles. However, due to the high lipid content of adipocytes and equipment limitations, TEM could not be pursued for this study. In our experiments, we inhibited Mini 202 uptake with Rose Bengal, an inhibitor of VMAT2 (IC_{50}=64 nM for 5-HT uptake). Rose Bengal also inhibits the vesicular glutamate transporter (VGLUT) with an IC_{50} of 25 nM and the vesicular acetylcholine transporter (VAChT; another member of the solute carrier family 18) with an IC_{50} of >9700 nM.[15] VGLUT1 has been reported to be present in brown and white adipose tissue adipocytes.[33] VAChT expression in adipocytes has not been reported and neither has the ability of Mini 202 to bind VGLUT. Thus, it is possible that the Mini 202 uptake observed could be from Mini 202 binding at VGLUT, which is inhibited by Rose Bengal. We were unable to use the VMAT inhibitor tetrabenazine in our experiments due to the requirement that the drug be dissolved in 100% ethanol, which decreased the viability of the adipocytes during the experimental protocol. Comparison of the ability of Mini 202 to enter adipocytes of mice lacking VMAT could be a future experiment. There are limitations to genetic VMAT knock-out models as VMAT2−/− mice die a few days after birth.[34,35] The heterozygous mice survive but have reduced brain catecholamines.[34,35] In vivo imaging of VMAT activity in adipocytes by [^{11}C]tetranbenazine labeling combined with PET imaging[36] could be another way that VMAT function in adipocytes can be investigated.

It is possible that concentration by VMAT into vesicles is not the only mechanism by which adipocytes store NE. Exosomes isolated from adipocytes from visceral adipose tissue were recently found to be involved in intercellular signaling leading to liver pathogenesis.[37] Perhaps NE can also be packaged into exosomes or other extracellular vesicles for downstream effects on the vasculature.

Disease relevance of the findings

Why do adipocytes store NE?—PVAT adipocytes have high activity of the semicarbazide amine oxidase.[6] Thus, NE that is taken up into adipocyte vesicles would be protected from oxidation. Since NE is important for the induction of lipolysis of adipocytes,[38] storage of NE by the adipocyte and then release could be a way that adipocytes self-regulate lipolysis. It is interesting to consider the impact of these findings in disease.

Adipocyte biology is dysregulated in obesity.[39] If NE storage in adipocytes is impaired in obesity, less NE would be available for lipolysis. Measures of lipolysis – as an endpoint that could be affected by adipocyte stored NE- are beyond the scope of the intended study. However, the findings that adipocytes store NE remain to be investigated in obesity. Because PVAT is important for blood vessel function since it regulates its contractility and affects the inflammation of the vasculature, alterations in NE uptake and storage could also have profound effects on vascular tone.[40] A decrease in adipocyte uptake and storage of NE could increase contraction of vessels, thereby potentially increasing blood pressure.

Conclusion

The adrenergic system within the adipocyte has resemblances to that system best known in sympathetic neurons. Within the adipocytes exists mechanisms to synthesize, take up, metabolize and release NE.[3,5,6,7] We provide novel data supporting another adrenergic mechanism present in the adipocyte: NE storage through VMAT. These findings have large implications for the understanding of adipocyte as well as vascular biology. The question remains whether these mechanisms contribute to high blood pressure alterations in diseases such as obesity.

Supplementary Material

Refer to Web version on PubMed Central for supplementary material.

Acknowledgements

For her generous help in demonstrating the chromaffin cell isolation protocol, we thank Ms. Zuleirys Santana-Rodriguez of Dr. Arun Anantharam's lab at The University of Michigan.

Sources of Funding

This work was supported by NIH NHLBI P01HL70687 (SWW), NIH 2T32HL007974–16 (NA-L), NIH NRSA F31 HL128035–01 (NA-L), NIH GM111997 (AA), NIH NICHD R01 HD072968 (AJM), and the APS UGREF (MA).

Abbreviations and acronyms:

5-HT	5-hydroxytryptamine
APVAT	PVAT surrounding the thoracic aorta
DA	dopamine
MRPVAT	PVAT surrounding the mesenteric resistance vessels
MRV	mesenteric resistance vessels
NE	norepinephrine
NET	norepinephrine transporter
OCT3	organic cation transporter 3
PVAT	perivascular adipose tissue

RP	retroperitoneal
SERT	serotonin transporter
SI	signal intensities
SMA/V	superior mesenteric artery and vein
SMPVAT	PVAT surrounding the SMA/V
SVF	stromal-vascular fraction
TA	thoracic aorta
VMAT	vesicular monoamine transporter

References

1. Szasz T, Webb RC. Perivascular adipose tissue: More than just structural support. Clin Sci. 2012;122:1–12. [PubMed: 21910690]
2. Soltis EE, Cassis LA. Influence of perivascular adipose tissue on rat aortic smooth muscle responsiveness. Clin Exp Hypertens A. 1991;13:277–296. [PubMed: 2065467]
3. Vargovic P, Ukropec J, Laukova M, Cleary S, Manz B, Pacak K, Kvetnansky R. Adipocytes as a new source of catecholamine production. FEBS Lett. 2011;585:2279–2284. [PubMed: 21689652]
4. Ayala-Lopez N, Watts SW. New actions of an old friend: perivascular adipose tissue's adrenergic mechanisms. Br J Pharmacol. 2016;174:3454–3465. [PubMed: 27813085]
5. Ayala-Lopez N, Jackson WF, Burnett R, Wilson JN, Thompson JM, Watts SW. Organic cation transporter 3 contributes to norepinephrine uptake into perivascular adipose tissue. Am J Physiol-Heart Circ Physiol. 2015;309:H1904–H1914. [PubMed: 26432838]
6. Ayala-Lopez N, Thompson JM, Watts SW. Perivascular adipose tissue's impact on norepinephrine-induced contraction of mesenteric resistance arteries. Front Physiol. 2017;8.
7. Ayala-Lopez N, Martini M, Jackson WF, Darios E, Burnett R, Seitz B, Fink GD, Watts SW. Perivascular adipose tissue contains functional catecholamines. Pharmacol Res Perspect. 2014;2:e00041. [PubMed: 24904751]
8. Weihe E, Schafer MK-H, Erickson JD, Eiden LE. Localization of vesicular monoamine transporter isoforms (VMAT1 and VMAT2) to endocrine cells and neurons in rat. J Mol Neurosci. 1994;5:149–164. [PubMed: 7654518]
9. Intengan HD, Schiffrin EL. Structure and mechanical properties of resistance arteries in hypertension: role of adhesion molecules and extracellular matrix determinants. Hypertension. 2000;36:312–318. [PubMed: 10988257]
10. Watts SW, Shaw S, Burnett R, Dorrance AM. Indoleamine 2,3-diooxygenase in periaortic fat: mechanisms of inhibition of contraction. Am J Physiol Heart Circ Physiol. 2011;301:H1236–H1247. [PubMed: 21841011]
11. Contreras GA, Thelen K, Ayala-Lopez N, Watts SW. The distribution and adipogenic potential of perivascular adipose tissue adipocyte progenitors is dependent on sexual dimorphism and vessel location. Physiol Rep. 2016;4:e12993. [PubMed: 27738018]
12. Hull D The structure and function of brown adipose tissue. Br Med Bull. 1966; 22:92–96. [PubMed: 5321824]
13. Lee M, Gubernator NG, Sulzer D, Sames D. Development of pH-Responsive Fluorescent False Neurotransmitters. J Am Chem Soc. 2010;132:8828–8830. [PubMed: 20540519]
14. Ismail A, Ayala-Lopez N, Ahmad M, Watts SW. 3T3-L1 cells and perivascular adipocytes are not equivalent in amine transporter expression. FEBS Lett. 2017;591:137–144. [PubMed: 27926779]

15. Pietrancosta N, Kessler A, Favre-Besse F-C, Triballeau N, Quentin T, Giros B, Mestikawy SE, Acher FC. Rose Bengal analogs and vesicular glutamate transporters (VGLUTs). Bioorg Med Chem. 2010;18:6922–6933. [PubMed: 20708942]
16. Thelen K, Watts SW, Contreras GA. Adipogenic potential of perivascular adipose tissue preadipocytes is improved by coculture with primary adipocytes. Cytotechnology. 2018;70:1435–1445. [PubMed: 30051281]
17. Barcroft H, Edholm O, Mcmichael J, Sharpey-Schafer E. Posthæmorrhagic Fainting. The Lancet. 1944;243:489–491.
18. Matsuzawa Y, Shimomura I, Nakamura T, Keno Y, Kotani K, Tokunaga K. Pathophysiology and pathogenesis and visceral fat obesity. Obes Res. 1995;3:187S–194S. [PubMed: 8581775]
19. Chiba Y, Saitoh S, Takagi S, et al. Relationship between Visceral Fat and Cardiovascular Disease Risk Factors: The Tanno and Sobetsu Study. Hypertens Res. 2007;30:229–236. [PubMed: 17510504]
20. Despres J-P. Body Fat Distribution and Risk of Cardiovascular Disease: An Update. Circulation. 2012;126:1301–1313. [PubMed: 22949540]
21. Jeong JH, Chang JS, Jo Y-H. Intracellular glycolysis in brown adipose tissue is essential for optogenetically induced nonshivering thermogenesis in mice. Sci Rep. 2018;8:6672. [PubMed: 29704006]
22. Kuchii M, Shibata S, Mori J. Pharmacological nature of adrenergic innervation in rat aorta. Comp Gen Pharmac. 1973;4:131–138.
23. Nilsson H Different nerve responses in consecutive sections of the arterial system. Acta Physiol Scan. 1984;121:353–356.
24. Cantu RC and Goodman HM. Effects of denervation and fasting on white adipose tissue. Am J Physiol 1967;212:207–212. [PubMed: 6016006]
25. Camell CD, Sander J, Spadaro O, Lee A, Nguyen KY, Wing A, Goldberg EL, Youm YH, Brown CW, Elsworth J, Rodeheffer MS, Schultze JL, Dixit VD. Inflammasome-driven catecholamine catabolism in macrophages blunts lipolysis during ageing. Nature. 2017;550:119–123. [PubMed: 28953873]
26. Pirgalska RM, Seixas E, Seidman JS, et al. Sympathetic neuron associated macrophages contribute to obesity by importing and metabolizing norepineprhine. Nat Med. 2017;23:1309–1318. [PubMed: 29035364]
27. Fischer K, Ruiz HH, Jhun K, et al. Alternatively activated macrophages do not synthesize catecholamines or contribute to adipose tissue adaptive thermogenesis. Nat Med. 2017;23:623–630. [PubMed: 28414329]
28. Breining P, Pedersen SB, Pikelis A, Rolighed L, Sundelin EIO, Jessen N, Richelsen B. High expression of organic cation transporter 3 in human BAT-like adipocytes. Implications for extraneuronal norepinephrine uptake. Mol Cell Endocrinol. 2017;443:15–22. [PubMed: 28034777]
29. Wimalasena K Vesicular Monoamine Transporters: Structure-Function, Pharmacology, and Medicinal Chemistry. Med Res Rev. 2011;31:483–519. [PubMed: 20135628]
30. Erickson JD, Schafer MK, Bonner TI, Eiden LE, Weihe E. Distinct pharmacological properties and distribution in neurons and endocrine cells of two isoforms of the human vesicular monoamine transporter. Proc Natl Acad Sci USA. 1996;93:5166–5171. [PubMed: 8643547]
31. Gaskill PJ, Carvallo L, Eugenin EA, Berman JW. Characterization and function of the human macrophage dopaminergic system: implications for CNS disease and drug abuse. J Neuroinflammation. 2012;9.
32. Rudd ML, Nicolas AN, Brown BL, Fischer-Stenger K, Stewart JK. Peritoneal macrophages express the serotonin transporter. J Neuroimmunol. 2005;159:113–118. [PubMed: 15652409]
33. Nicolaysen A, Gammelsaeter R, Storm-Mathisen J, Gundersen V, Iversen PO. The components required for amino acid neurotransmitter signaling are present in adipose tissues. J Lipid Res. 2007;48:2123–2132. [PubMed: 17600303]
34. Fon EA, Pothos EN, Sun B, Killeen N, Sulzer D, Edwards RH. Vesicular Transport Regulates Monoamine Storage and Release but Is Not Essential for Amphetamine Action. Neuron. 1997;19:1271–1283. [PubMed: 9427250]

35. Takahashi N, Miner LL, Sora I, Ujike H, Revay RS, Kostic V, Jackson-Lewis V, Przedborski S, Uhl GR. VMAT2 knockout mice: Heterozygotes display reduced amphetamine-conditioned reward, enhanced amphetamine locomotion, and enhanced MPTP toxicity. Proc Natl Acad Sci USA. 1997;94:9938–9943. [PubMed: 9275230]

36. DaSilva JN, Kilbourn MR. In vivo binding of [11C]tetrabenazine to vesicular monoamine transporters in mouse brain. Life Sci. 1992;51:593–600. [PubMed: 1640810]

37. Koeck ES, Iordanskaia T, Sevilla S, Ferrante SC, Hubal MJ, Freishtat RJ, Nadler EP. Adipocyte exosomes induce transforming growth factor beta pathway dysregulation in hepatocytes: a novel paradigm for obesity-related liver disease. J Surg Res. 2014;192:268–75. [PubMed: 25086727]

38. Bartness TJ, Liu Y, Shrestha YB, Ryu V. Neural Innervation of White Adipose Tissue and the Control of Lipolysis. Front Neuroendocrinol. 2014;35:473–493. [PubMed: 24736043]

39. Van de Voorde J, Boydens C, Pauwels B, Decaluwe K. Perivascular adipose tissue, inflammation and vascular dysfunction in obesity. Curr Vasc Pharmacol. 2014; 12:403–11. [PubMed: 24846230]

40. Szasz T, Bomfim GF, Webb RC. The influence of perivascular adipose tissue on vascular homeostasis. Vasc Health Risk Manag. 2013;9:105–116. [PubMed: 23576873]

Highlights

- Perivascular adipose tissue (PVAT) surrounding the thoracic aorta, superior mesenteric artery and vein, and mesenteric resistance vessels contain norepinephrine (NE).
- These PVATs also express the vesicular monoamine transporters: VMAT1 and VMAT2.
- A storage mechanism for NE in PVAT adipocytes is likely OCT3-, NET-, and VMAT-dependent.
- In comparison to other adipocytes, perivascular adipocytes may be unique in their ability to store NE by means of VMAT.

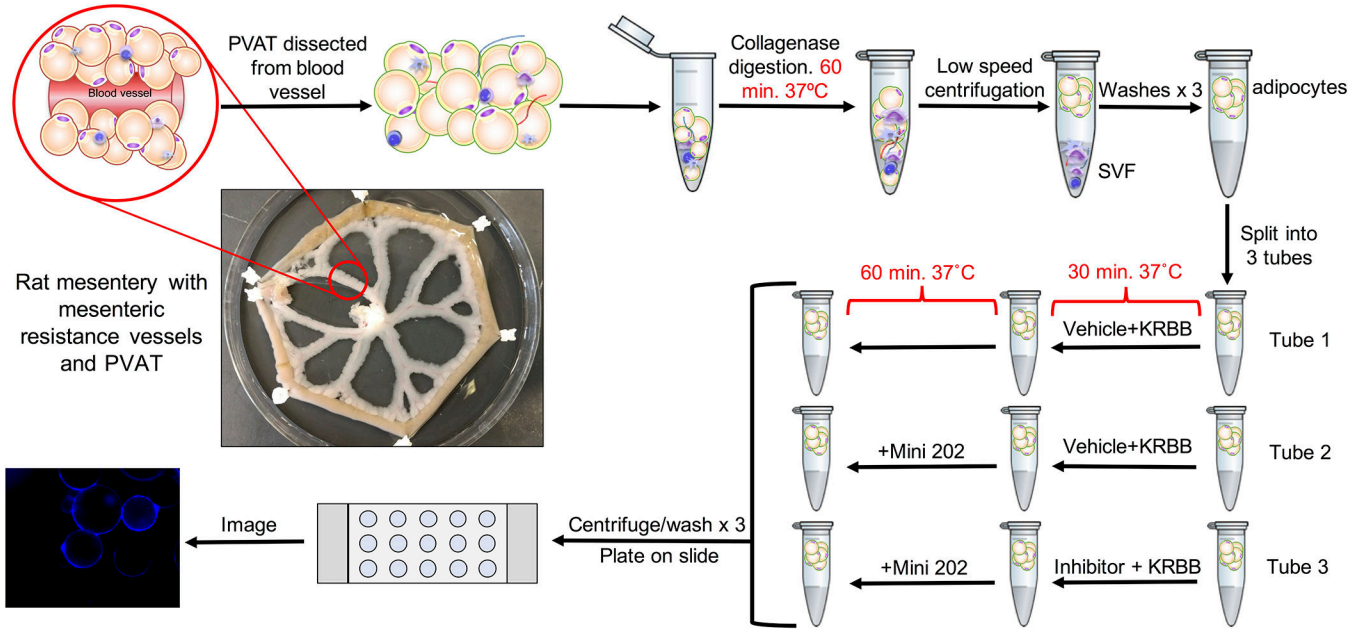

Figure 1.
Mini 202 experimental protocol.

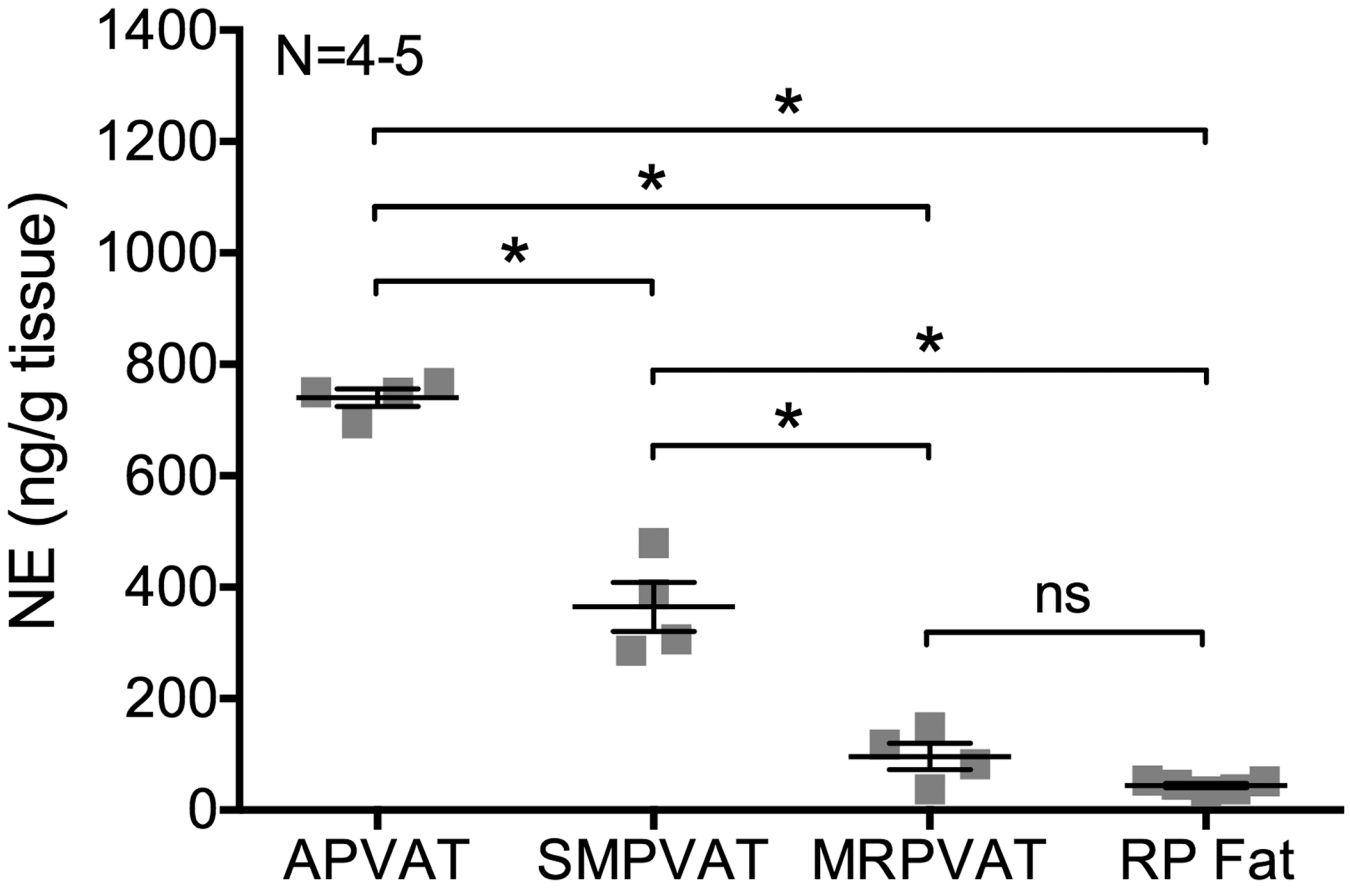

Figure 2.

Thoracic aortic (A), superior mesenteric (SM), and mesenteric (MR) PVATs contain norepinephrine (NE). HPLC measures for NE content in APVAT, SMPVAT, MRPVAT, and retroperitoneal (RP) fat. Bars represent mean ± SEM for paired tissues from 4–5 animals, represented by squares. ns= not significant. *= $p<0.0001$ by a one-way ANOVA.

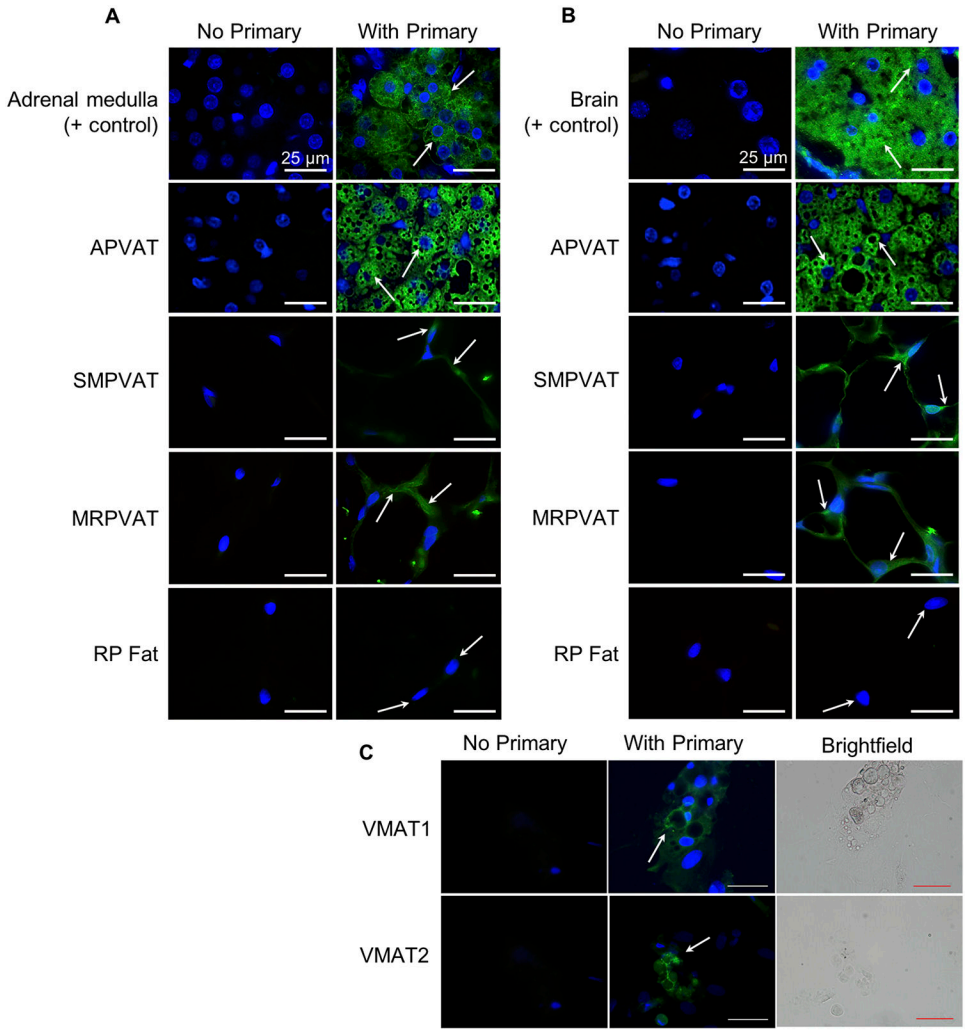

Figure 3.

VMAT1 and VMAT2 are present in aortic (A, 2nd rows), superior mesenteric (SM, 3rd rows) and mesenteric (MR, 4th rows) PVATs, but not retroperitoneal fat (RP fat, bottom rows). **A** and **B**.

Immunofluorescence images using a primary antibody against VMAT1 **(A)** or VMAT2 **(B)** on right and negative control image for each tissue on left. Images were taken with a 100× oil objective. Arrows indicate areas of interest/positive staining (green). All scale bars represent 25 µm. Representative of 4–6 animals. Positive control tissues (top rows) were rat adrenal medulla **(A)** and the anterior commissure of the rat brain **(B)**. VMAT1 and VMAT2 staining is present in adipocytes differentiated from adipocyte precursors in MRPVAT SVF **(C)**. Scale bars represent 50 µm. Representative of 3 animals.

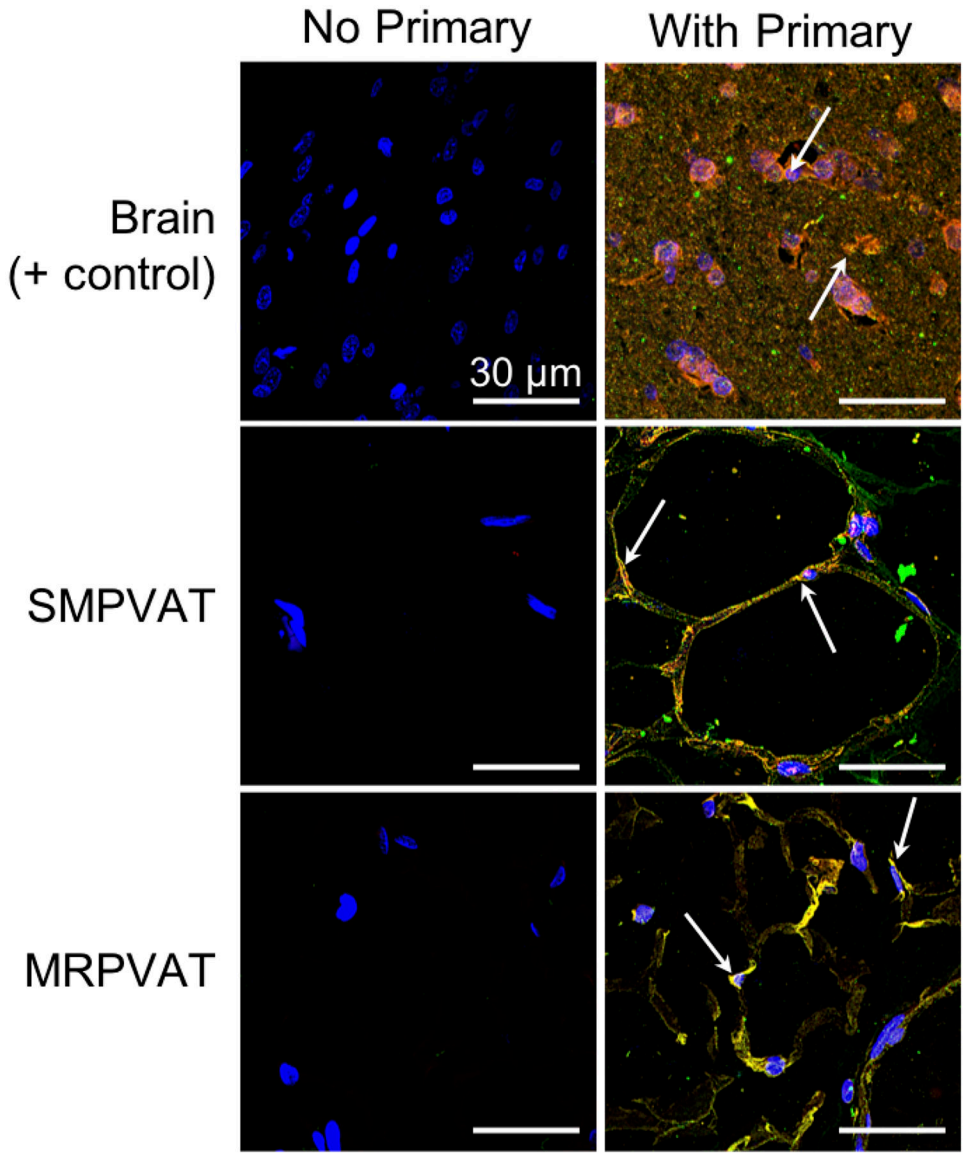

Figure 4.

VMAT2 and NE co-localize in superior mesenteric (SM, middle) and mesenteric (MR, bottom) PVATs. Immunofluorescence Z-stack images with primary antibodies against VMAT2 (red) and NE (green) on the right and negative control image for each tissue on the left. Images were taken with a 120× oil objective on a confocal microscope. Arrows indicate areas of positive staining. All scale bars represent 30 µm. Representative of 4 animals. Positive control tissue (top) was the caudate putamen region of the rat brain.

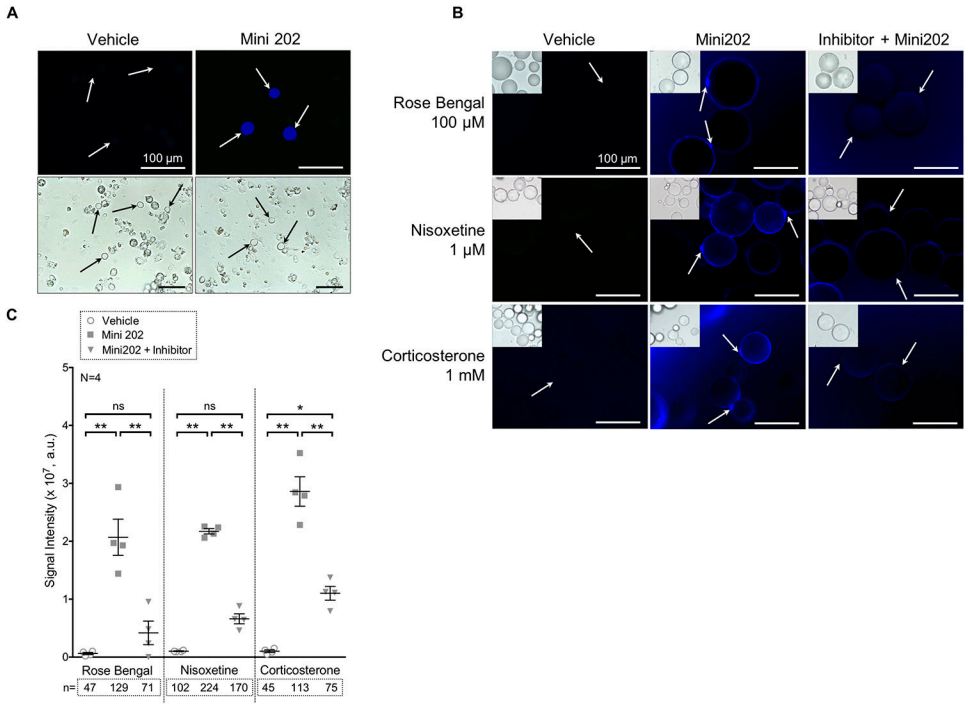

Figure 5.

Mini 202 uptake in mesenteric PVAT adipocytes is VMAT-, NET-, and OCT3-dependent. **(A)** Images of the Mini 202 positive control: rat adrenal medulla chromaffin cells. Vehicle on left and Mini 202 condition on right. Fluorescent images (top row) with corresponding brightfield images (bottom row). Images were taken with a 40× objective. Arrows indicate healthy (non-granulous) chromaffin cells that have taken up Mini 202. All scale bars represent 100 µm. **(B)** Fluorescent images of vehicle (left), Mini 202 (middle), and Inhibitor + Mini 202 (right) for the three inhibitors: Rose Bengal (top), nisoxetine (middle), and corticosterone (bottom). Images were taken with a 40× objective. Arrows indicate areas of interest. All scale bars represent 100 µm. Brightfield image inset for reference. **(C)** Quantification of Mini 202 fluorescence when taken up by MRPVAT adipocytes. Fluorescence was decreased by treatment with VMAT inhibitor (Rose Bengal), and inhibitors of plasma membrane transporters NET (nisoxetine) and OCT3 (corticosterone). n values below graph indicate the number of cells quantified in duplicate (i.e. the average number of cells quantified by each researcher). a.u. indicates arbitrary units of signal intensity. Bars represent mean ± SEM for four biological replicates (N=4). * p=0.0013, and ** p<0.0001 by a one-way ANOVA.

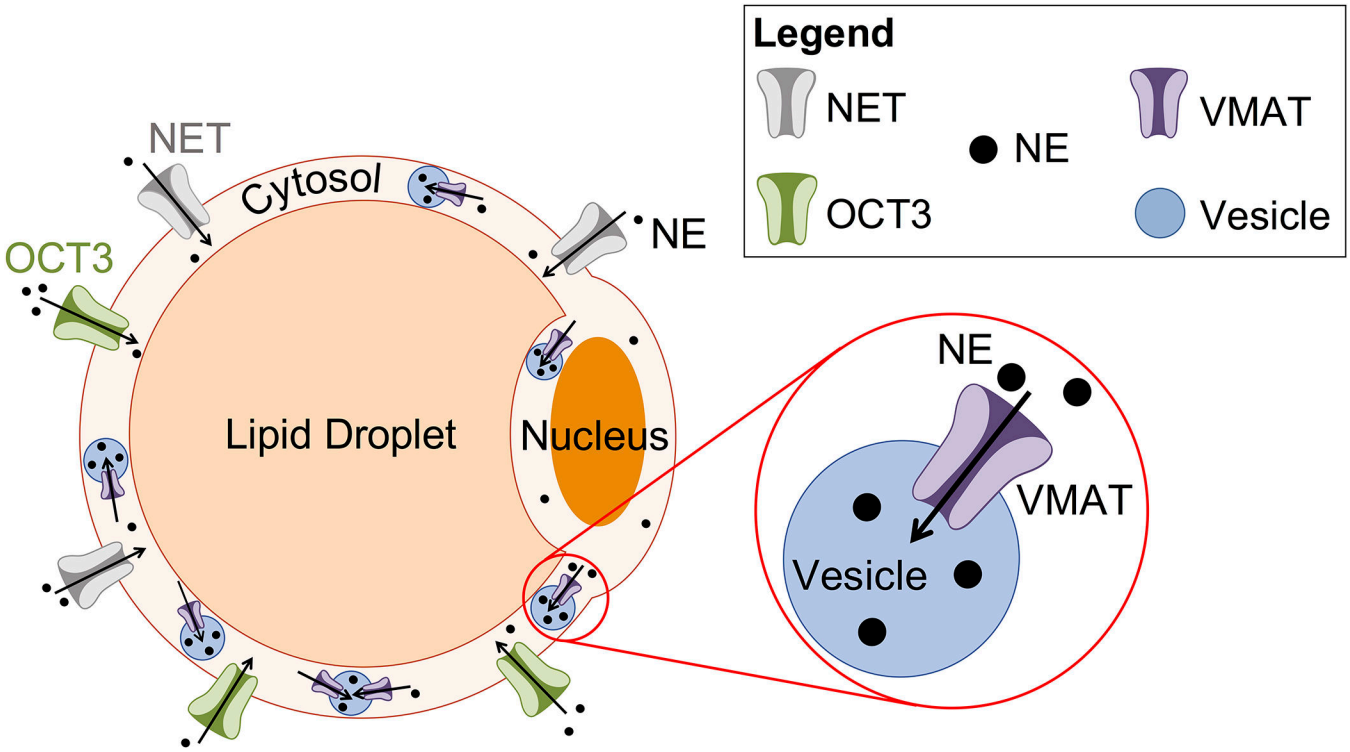

Figure 6.

Proposed NE storage mechanism in PVAT adipocytes. NE enters the cell through the plasma membrane transporters OCT3 and NET. NE is stored in vesicles within the cytoplasm by VMAT. Diagram not to scale.

Table 1

VMAT1 and VMAT2 mRNA expression in MRPVAT adipocytes (top) and SVF (bottom) separated from the same animal. Normalization of VMAT to ACTB is expressed as $2^{-\text{delta CT.}}$ Representative of four (4) different rats.

Genes	Average C_T of detected	C_T of positive control	Normalization (VMAT/ACTB)
Adipocytes			
ActB (ACTB)	18.49 ± 0.12	Adrenal: 17.18 LC: 21.31	
Slc18a1 (VMAT1)	35.00 ± 0.88	Adrenal: 24.46	$1.92\pm0.94\times10^{-6}$
Slc18a2 (VMAT2)	30.96 ± 0.01	LC: 26.95	$1.73\pm0.13\times10^{-4}$
SVF			
ActB (ACTB)	19.75±0.25	Adrenal = 18.60 LC = 19.21	
Slc18a1 (VMAT1)	37.30±0.30	Adrenal = 24.24	$5.73\pm1.26\times10^{-6}$
Slc18a2 (VMAT2) Normalized to ActB	28.48±0.30	LC = 22.66	$2.42\pm0.3\times10^{-4}$

C_T indicates threshold cycle. Adrenal and locus coeruleus (LC) were used as positive controls. Beta-actin (ACTB) was the housekeeping gene.